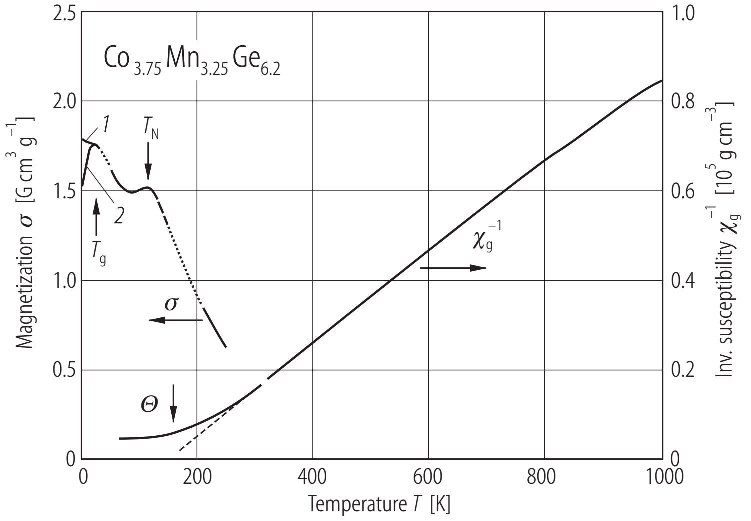

Fig. 109. $Co_{3.75}Mn_{3.25}Ge_{6.2}$. Temperature dependence of the mass magnetization σ in a magnetic field H = 9.0 kOe, as well as the inverse magnetic mass susceptibility χ_g^{-1}. Measurements were carried out on heating, after cooling from 80 K to 4.2 K (*1*) in a field of 9.5 kOe and (*2*) in zero field [92H1].

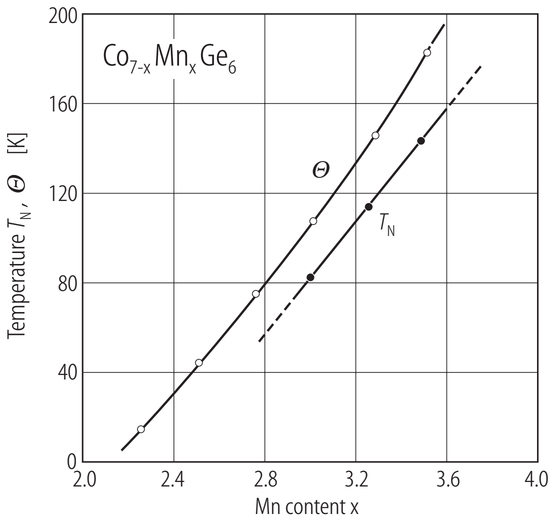

Fig. 110. $Co_{7-x}Mn_xGe_6$. Composition dependence of Néel temperature T_N and the paramagnetic Curie temperature Θ [92H1].

1.5.4.7 MM'X ternary compounds

The investigations on the ternary MM'X compounds or on the related $MM'X_{1-x}X'_x$ compounds, where M and M' are different 3d elements and X and X' 4B element, include the effect of pressure on the magnetism of the pure Mn compounds.

Survey

	Composition x	Properties	Figure	Table
$MnCoSi_xGe_{1-x}$	0.1	$T_C(p)$	111	
	0...0.4, 0.7...1	$(1/T_C)dT_C/dp$	112	
$MnNiSi_xGe_{1-x}$	0.05	*p*-*T* magnetic phase diagram	113	
	0.2	$M(H;p)$	114	
	0.2	*p*-*T* magnetic phase diagram	115	
$Ti_{0.05}Mn_{0.95}NiGe$		*p*-*T* magnetic phase diagram	116	
$TiCo_xNi_{1-x}Sn$	0.1...1	$\chi_m^{-1}(T)$	117	
	0...1	$p_{m,eff}(x)$, $p_m(x)$	118	
TiCoSn		$\rho(H)$	119	
		a, T_C, Θ, p_m		11

Table 11. Supplement to Table 13 in LB III/19C, subsect. 1.5.4.7. Magnetic and related properties of MM'X compound TiCoSn [94P1].

	TiCoSn
Crystal structure	cubic, $C1_b$ (MgAgAs)
a [Å]	5.997
Magnetism	ferro
T_C [K]	134
Θ [K]	176
p_m [μ_B/f.u.]	0.357 at 0 K
$p_{m,eff}$ [μ_B/f.u.]	1.25

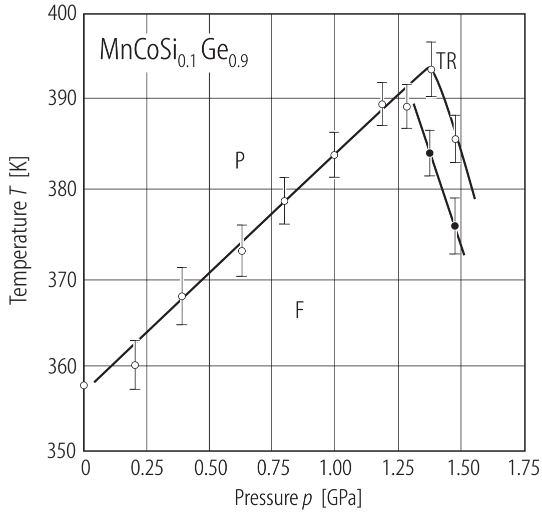

Fig. 111. $MnCoSi_{0.1}Ge_{0.9}$. Magnetic phase diagram in a pressure - temperature plane (P: paramagnet, F: ferromagnet). The Curie point is defined arbitrarily by the inflection point of the ac initial susceptibility curve against temperature [89N1]. For p >1.3 GPa, a magneto-structural transition (with hysteresis) to the hexagonal paramagnet is observed (open circles: increasing temperature, solid circles: decreasing temperature). TR: triple point. 1 GPa = 10 kbar.

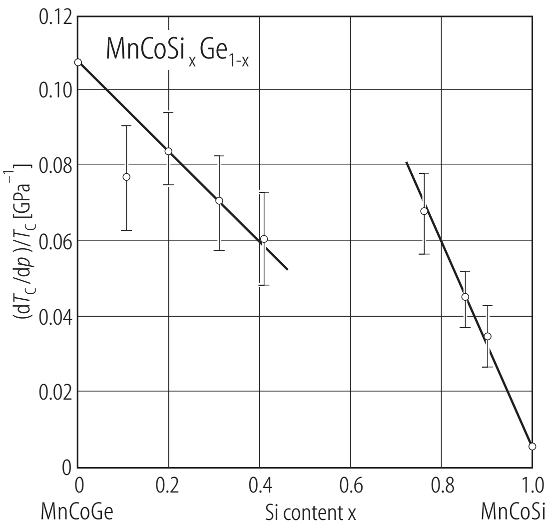

Fig. 112. $MnCoSi_xGe_{1-x}$. Composition dependence of the rate of change of the Curie temperature T_C by pressure p, $(1/T_C)dT_C/dp$ [89N1]. 1 GPa = 10 kbar.

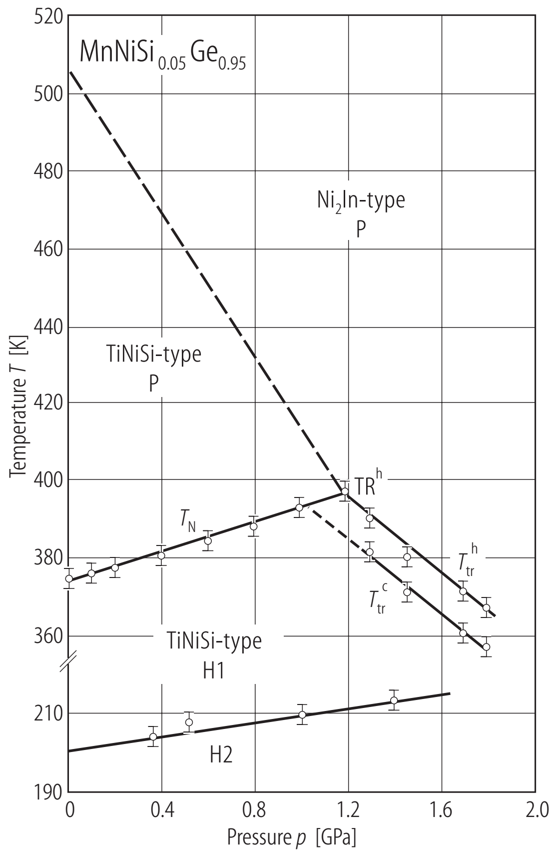

Fig. 113. $MnNiSi_{0.05}Ge_{0.95}$. Magnetic phase diagram in a pressure - temperature plane [88D1]. The magnetic transition temperature was determined from ac initial susceptibility vs. temperature curve as in Fig. 111. Superscripts h and c stand for heating and cooling, respectively. P: paramagnet; H1: simple spiral; H2: cycloidal spiral; TR: triple point. 1 GPa = 10 kbar.

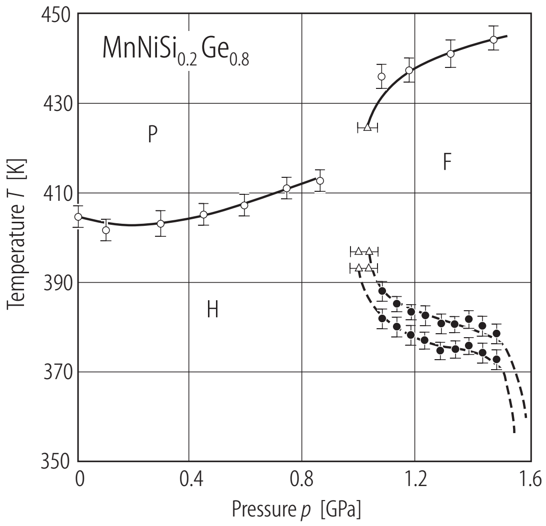

Fig. 115. $MnNiSi_{0.2}Ge_{0.8}$. Partial magnetic phase diagram in a pressure - temperature plane. The magnetic transition temperature was derived from ac initial susceptibility vs. temperature curves as in Fig. 111, except for the data shown by triangles which are derived from isothermal measurements [88D1]. P: paramagnet; F: (noncollinear) ferromagnet; H: helical. 1 GPa = 10 kbar.

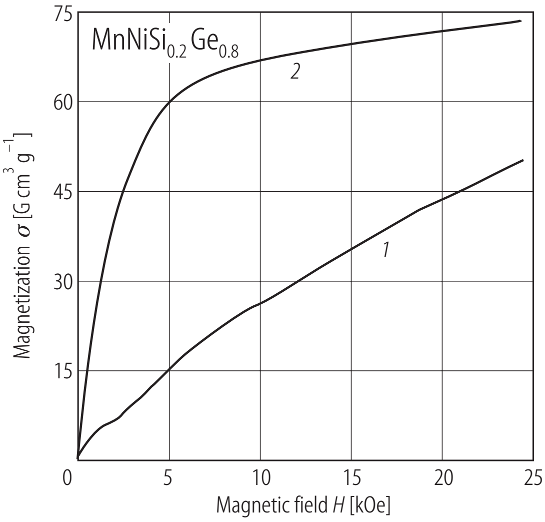

Fig. 114. $MnNiSi_{0.2}Ge_{0.8}$. Dependence of the mass magnetization σ on a magnetic field H: (*1*) under atmospheric pressure at 295 K, and (*2*) under a pressure of 1.5 GPa at 399 K [88D1]. 1 GPa = 10 kbar.

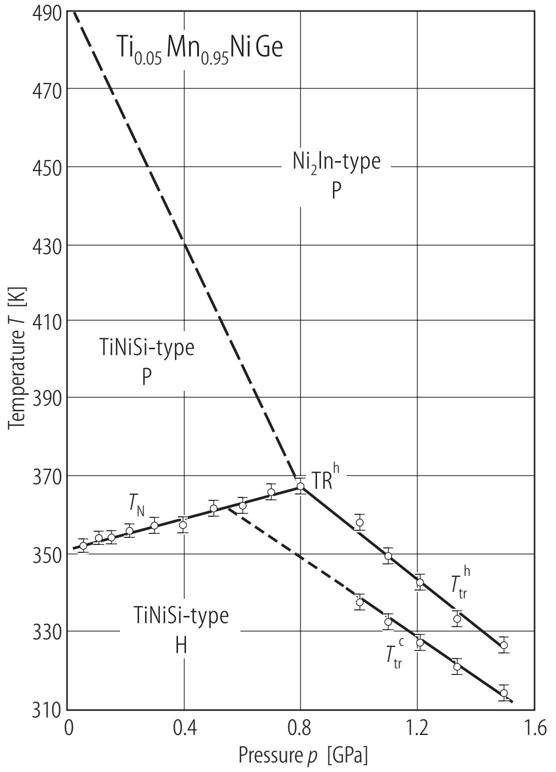

Fig. 116. $Ti_{0.05}Mn_{0.95}NiGe$. Magnetic phase diagram in a pressure - temperature plane. The magnetic transition temperature was determined from ac initial susceptibility vs. temperature curve, as its maximum at lower pressure or as its inflection points at higher pressure. The latter with a hysteresis of about 10 K is a magneto-structural transition of first order [88D1]. The superscripts h and c stand for heating and cooling, respectively. TR means triple point. P: paramagnet; H: helical (simple spiral). 1 GPa = 10 kbar.

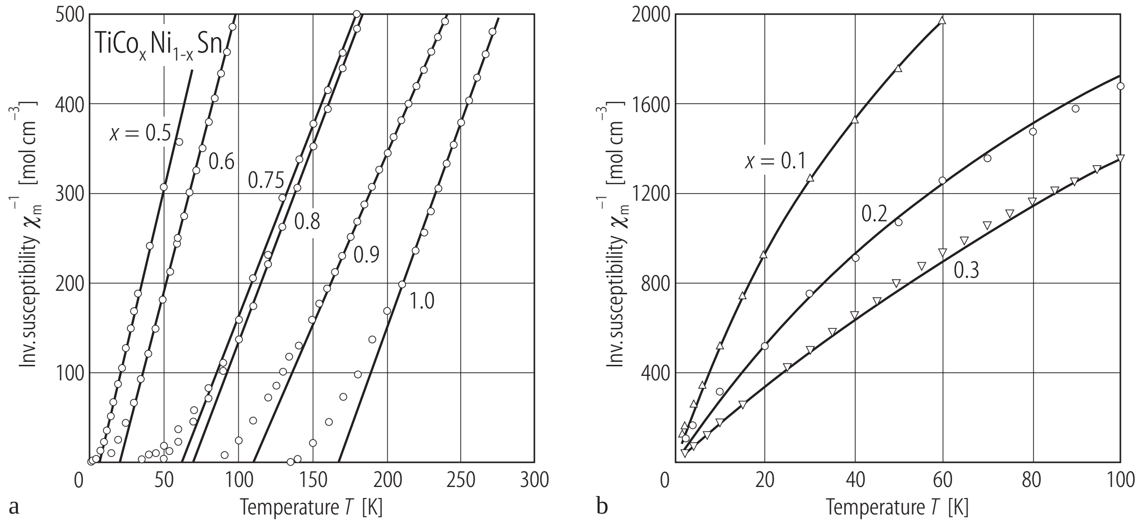

Fig. 117. $TiCo_xNi_{1-x}Sn$. Temperature dependence of the reciprocal molar magnetic susceptibility χ_m^{-1}. Some irregular spacing of the curves in (**a**) was attributed to deviation of the composition from the nominal one. The curves in (**b**) are fits to the expression $\chi = \chi_0 + C/(T - \Theta)$ [94P1].

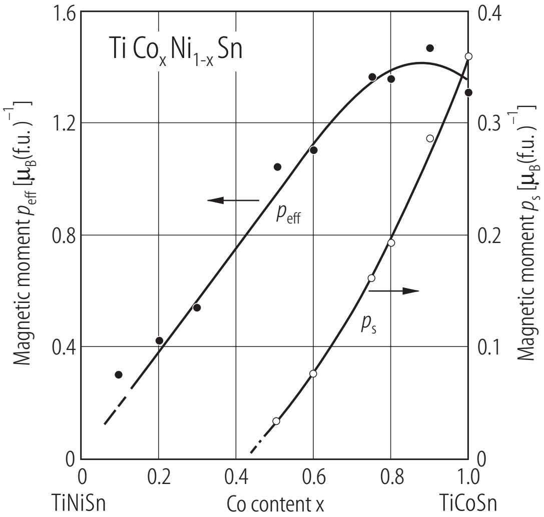

Fig. 118. $TiCo_xNi_{1-x}Sn$. Composition dependence of the effective magnetic moment and of the spontaneous magnetic moment per formula unit [94P1].

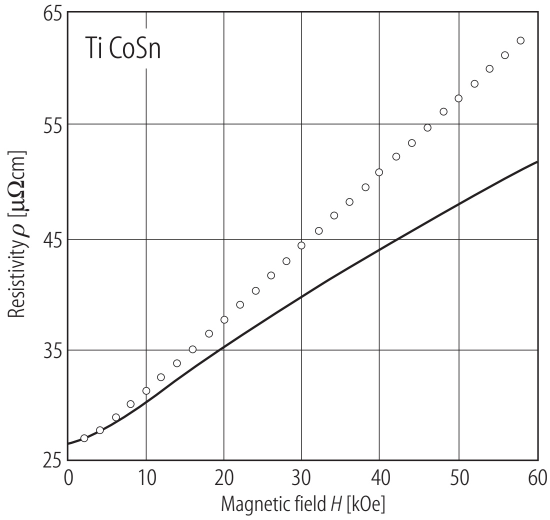

Fig. 119. TiCoSn. Dependence of the electrical resistivity ρ at 1.6 K on an applied magnetic field H parallel (continuous curve) or perpendicular (open circles) to the electric current [94P1].

1.5.4.8 References for 1.5.4

General references

58p Pearson, W.B.: A Handbook of Lattice Spacings and Structures of Metals and Alloys, London: Pergamon Press (1958).
90m Massalski, T.B. (editor-in-chief): Binary Alloy Phase Diagrams, 2nd ed. (in 3 volumes), Ohio: ASM International (1990).
91v Villars, P., Calvert, L.D.: Pearson's Handbook of Crystallographic Data for Intermetallic Phases, 2nd ed. (in 4 volumes), Ohio: ASM International (1991).
92b Brandes, E.A., Brook, G.B. (editors): Smithells Metals Reference Book, 7th ed., Oxford: Butterworth-Heinemann (1992).

Special references

63W1 Watanabe, H., Yamamoto, H., Ito, K.: J. Phys. Soc. Jpn. **18** (1963) 995.
67J1 Jaccarino, V., Wertheim, G.K., Wernick, J.H., Walker, L.R., Arajs, S.: Phys. Rev. **160** (1967) 476.
67R1 Richardson, M.: Acta Chem. Scand. **21** (1967) 2305, through [78F1].
71D1 Dusausoy, Y., Protas, J., Wandji, R., Roques, B.: Acta Crystallogr., Sect. B **27** (1971) 1209 (in French).
71K1 Kádár, G., Krén, E.: Int. J. Magn. **1** (1971) 143.
72F1 Fruchart, E., Lorthioir, G., Fruchart, R.: C.R. Seances Acad. Sci. (Paris) Ser. C **275** (1972) 1415 (in French).
72F2 Fukamichi, K., Saito, H.: J. Phys. Soc. Jpn. **33** (1972) 1485.
73M1 Moriya, T., Kawabata, A.: J. Phys. Soc. Jpn. **34** (1973) 639; **35** (1973) 669.
78F1 Forsyth, J.B., Wilkinson, C., Gardner, P.: J. Phys. F (UK) **8** (1978) 2195.
78F2 Fruchart, D., Bertaut, E.F.: J. Phys. Soc. Jpn. **44** (1978) 781.
78Y1 Yasuoka, H., Jaccarino,V., Sherwood, R. C., Wernick, J. H.: J. Phys. Soc. Jpn. **44** (1978) 842.
79M1 Moriya, T.: J. Magn. Magn. Mater. **14** (1979) 1.